Food & Function

ROYAL SOCIETY OF CHEMISTRY

PAPER

View Article Online
View Journal | View Issue

Cite this: *Food Funct.*, 2025, **16**, 2347

Bifidobacterium animalis subsp. *lactis* BLa80 alleviates constipation in mice through modulating the stem cell factor (SCF)/c-Kit pathway and the gut microbiota†

Zhaochun Zhang,[a] Jie Li,[a] Ziyi Wan,[a] Shuguang Fang,[c] Yunjiao Zhao,[c] Qian Li *[b] and Min Zhang *[a,b]

Probiotics, as health ingredients, have attracted widespread attention. However, due to the wide variety of probiotic species, their laxative effects and the underlying mechanisms remain elusive. In this study, we investigated the laxative effect of *Bifidobacterium animalis* subsp. *lactis* BLa80 (at concentrations of 1.0×10^8, 2.0×10^8, and 4.0×10^8 CFU per mL, with a dosage of 0.2 mL each) in mice, utilizing a functional constipation mouse model induced with loperamide hydrochloride (0.2 mL, 10 mg per kg BW) for 7 consecutive days. Meanwhile, a blank group (treated with 0.2 mL of 0.9% saline) and a positive control group (treated with mosapride at a dose of 5 mg per kg BW) were also set up. The body weight, fecal water content, intestinal propulsion rate, colon tissue histology, fecal microbial composition, serum indices, and colon mRNA levels of the mice were measured, employing histological and biochemical assays, GC-MS, RT-qPCR and 16S rRNA gene sequencing *etc*. Results showed BLa80 could accelerate intestinal peristalsis, maintain fecal moisture, prevent intestinal barrier disruption, increase short-chain fatty acid production, prevent gut microbe dysbiosis and constipation in mice. It also helped to keep the levels of 5-hydroxytryptamine (5-HT), motilin (MTL), and substance P (SP) normal, up-regulated the mRNAs of intestinal mucin 2 (MUC2), stem cell factor (SCF), and the tyrosine kinase receptor c-Kit, and down-regulated the mRNA of aquaporins (AQPs), especially at a high-dose. This study indicated that BLa80 held the potential to emerge as a novel ingredient in functional foods designed for constipation relief and as a treatment alternative.

Received 22nd December 2024,
Accepted 4th February 2025

DOI: 10.1039/d4fo06350c

rsc.li/food-function

Introduction

Constipation is a highly prevalent gastrointestinal disorder globally, affecting all age groups.[1] The World Gastroenterology Organization's survey indicates that around a quarter of worldwide consumers experience digestive problems. The incidence of chronic constipation is notably high, up to 20% overall, 50% among the elderly, with 67% prevalence in those over 65.[2] It can cause discomfort, pain, and difficulties in defecation.[3] Frequent or chronic constipation may lead to depression, cardiovascular disease, irritable bowel syndrome (IBS), hepatic encephalopathy, abdominal hernia, and increase colorectal cancer risk.[4] Currently, constipation treatment is mainly pharmacological, including 5-HT4 receptor agonists as prokinetic agents, lubiprostone and linagliptin as intestinal prosecretory agents, and laxatives like senna, bisacodyl, and magnesium.[5] However, most medications may cause drug dependence, diarrhea, and potential damage to the enteric nervous system due to long-term toxic side effects and adverse reactions.[6] Thus, finding safer and more effective therapies for constipation relief is crucial.

In recent years, a multitude of studies have unearthed a profound association between gut microbiota alterations and constipation occurrence. The relationship between the gut microbiota and constipation is complex and multifaceted, not a simple cause-and-effect association but a sophisticated interplay of various microbial species and their metabolites within the gut ecosystem.[7] For instance, certain microbial metabolites may modulate neurotransmitters secretion and activity involved in gut motility regulation, affecting intestinal propulsion rate.[8] Moreover, gut microbiota composition could also

[a]*State Key Laboratory of Food Nutrition and Safety, College of Food Science and Engineering, Tianjin University of Science and Technology, Tianjin 300457, China. E-mail: zm0102@tust.edu.cn*
[b]*Nutritious and Healthy Food Sino-Thailand Joint Research Center, Tianjin Agricultural University, Tianjin 300392, China. E-mail: limengqia@163.com*
[c]*Wecare Probiotics Co., Ltd, Suzhou, Jiangsu Province 215200, China*
† Electronic supplementary information (ESI) available. See DOI: https://doi.org/10.1039/d4fo06350c

impact gut barrier integrity and function, influencing water and electrolytes absorption, crucial in constipation development. Additionally, gut microbiota imbalance may lead to pathogenic or opportunistic microorganisms overgrowth, producing toxins or substances that disrupt the enteric nervous system and exacerbate constipation.[9]

Constipation may potentially be linked to gut–brain axis regulation. The gut–brain axis, which connects the enteric nervous system (ENS) of the gastrointestinal tract with the central nervous system (CNS), assumes a crucial function in maintaining the body's homeostasis, including the regulation of essential physiological processes like digestion and appetite.[10] Gastrointestinal hormones, serve as vital mediators within this axis. For illustration, 5-HT, a pivotal neurotransmitter synthesized by intestinal chromaffin cells, has multiple gut functions, like modulating peristalsis, smooth muscle contraction, and mucosal secretion. In the gut–brain axis, 5-HT signals travel bidirectionally between the gut and brain. For example, gut microbiota modifications can affect gut 5-HT production, influencing brain behavioral patterns. Additionally, the brain can regulate gut 5-HT release *via* the autonomic nervous system.[11]

Genes related to constipation, namely aquaporins (AQPs), intestinal mucin 2 (MUC2), stem cell factor (SCF), and the tyrosine kinase receptor c-Kit, have significant roles in constipation-related physiological processes. AQPs, involved in transmembrane water transport, affect intestinal hydration and fluid balance, contributing to constipation.[12] MUC2 encodes mucin 2, a crucial part of the intestinal mucus layer for barrier function and lubrication; its expression changes may lead to constipation.[13] Interstitial cells of cajal (ICC), neural-like cells at motor neuron ends, mediate neurotransmitter production and function. Abnormal ICCs are linked to gastrointestinal dyskinesia. ICCs express c-Kit and its ligand SCF, which is vital for cell growth and exerts functions mainly *via* binding to c-Kit. The SCF/c-Kit signaling pathway is crucial for ICC's normal development, maturation, and phenotype maintenance.[14] Dysregulation of these genes may cause or worsen constipation.

Clinical investigations have identified pronounced discrepancies in the intestinal microbiota's structure between healthy subjects and those with constipation. It's clear that the diverse bacteria in constipated patients' intestines can greatly affect intestinal motility.[15] Dysbiosis, a microbial equilibrium perturbation, furthermore perturbs metabolites composition, specifically short-chain fatty acids (SCFAs) and tryptophan catabolite metabolites.[13] SCFAs can ameliorate constipation by escalating serotonin levels, stimulating mucosal receptors, and directly interacting with the intestinal smooth muscle. Gut microbes implicated in constipation pathophysiology may also disrupt the microflora.[16] These microbes participate in gastrointestinal hormones biosynthesis, potentially to alleviating constipation by augmenting gastrointestinal motility.[17] Thus, intestinal imbalance emerges as a potentially pivotal risk factor for constipation onset and persistence.

The utilization of probiotics for constipation alleviation has emerged as a prominent research focus and holds the potential to be a secure and efficacious approach. Notably, *Bifidobacterium animalis* has been prevalently employed as an intestinal microecological agent.[18] Numerous studies have shown that *Bifidobacterium animalis* can improve the intestinal microenvironment by increasing short-chain fatty acid (SCFA) production, enhancing colon water and electrolyte absorption, softening stools, and facilitating bowel movements to relieve constipation.[19] Moreover, it has been found to enhance enteric nervous system function by stimulating the release of neurotransmitters like acetylcholine involved in gut motility regulation, thus promoting intestinal smooth muscle contraction and accelerating intestinal transit time.[20] Some experiments also indicate that it can regulate gut immune responses, reducing inflammation related to constipation and contributing to bowel function normalization through modulating intestinal immune cells and cytokines.[21] Another important aspect is that *Bifidobacterium animalis* can compete with gut pathogens, and this competitive exclusion mechanism helps maintain a healthy gut microbiota balance essential for proper digestion and defecation.[22] Furthermore, long-term clinical trials have shown that patients regularly consuming its supplements have a reduced constipation frequency and improved bowel movement regularity, with more normal stool consistency, indicating a positive effect on constipation relief and suggesting it could be a reliable and sustainable option for constipation management.[23] BLa80, a subspecies of *Bifidobacterium animalis* isolated from breast milk samples collected in the Hongyuan pastoral area of Sichuan, China, has demonstrated effectiveness in alleviating gastrointestinal symptoms in clinical studies.[24] However, its mechanism of action remains unclear.

To elucidate the efficacy and the fundamental mechanisms by which BLa80 acts upon loperamide-induced constipation in BALB/c mice, a comprehensive assessment was carried out regarding the gastrointestinal motility, gastrointestinal regulatory peptides, the content of SCFAs, expression of the stem cell factor (SCF)/c-kit signaling pathway, and the characteristics of the colon and fecal microbiot. This evaluation was conducted from the perspective of "Interstitial cells of cajal (ICC) cell-mouse-microbiota". Through this multi-faceted analysis, this study not only presented a novel means for alleviating constipation but also suggested that BLa80 could potentially be a novel and valuable ingredient in functional foods designed to address constipation. Moreover, it might emerge as a promising alternative in the therapeutic strategies for constipation management.

Materials and methods

Chemicals

Bifidobacterium animalis subsp. *lactis* BLa80 was procured from Wecare Probiotics Co., Ltd (Suzhou, China). The De Man–Rogosa–Sharpe (MRS) agar was furnished by Hopebiol Co., Ltd (Qingdao, China). The basic dietary formulated feed was obtained from SPF (Beijing) Biotechnology Co., Ltd, Beijing,

China. This particular feed was composed of 18.0% crude protein, 4.0% crude fat, 5.0% crude fiber, with calcium content ranging from 1.0% to 1.8%, phosphorus content from 0.6% to 1.2%, 10.0% moisture, and 8.0% crude ash. Unless otherwise specified, all other chemicals utilized were of analytical grade, meeting the requisite standards for experimental and analytical applications.

Bacteria preparation and cultivation

Under sterile conditions, the BLa80 freeze-dried bacterial powder was dissolved in normal saline. Subsequently, the dissolved bacterial solution was aseptically inoculated into MRS broth medium and then incubated under strictly anaerobic conditions at a precisely regulated temperature of 37 °C for an incubation duration of 24 hours. Subsequently, the resultant fermentation broth was subjected to centrifugation at a rotational velocity of 8000 rpm for a duration of 5 minutes at a low temperature of 4 °C. The harvested cells were meticulously washed thrice with sterile saline and subsequently adjusted to the specific concentrations of 1.0×10^8 CFU per mL, 2.0×10^8 CFU per mL and 4.0×10^8 CFU per mL, respectively.[25,26] It is of particular importance to note that the bacterial suspensions intended for mouse gavage were freshly prepared on a daily basis to ensure optimal viability and experimental reproducibility.

Animal and experimental design

Seventy-two male specific pathogen free (SPF) Balb/c mice weighing 18 ± 2.0 g were furnished by SPF (Beijing) Biotechnology Co., Ltd (Beijing, China, certificate number: SCXK Jing 2019-0010). The mice were accommodated in the premises of Tianjin University of Science and Technology, kept under a 12-hour light–dark cycle at 23 ± 1 °C and furnished with unrestricted access to food and water. After a one-week acclimation phase, the mice were randomly sorted into six groups, each containing 12 mice, namely: the blank control group (BC), the model group (M), the positive control group (PC), the BLa80 low-dose group (BLa80-L), the BLa80 medium-dose group (BLa80-M), and the BLa80 high-dose group (BLa80-H). During the entire experiment, the BC group was given daily saline gavage. With the exception of the BC group, all mice were gavaged with 10 mg per kg BW loperamide hydrochloride once daily to generate constipation, and this modeling procedure endured for one week. Upon completion of the modeling, the M group was gavaged daily with saline, the PC group was gavaged with 5 mg per kg BW mosapride citrate tablets, and the BLa80-L, BLa80-M, and BLa80-H groups were respectively administered 1.0×10^8 CFU per mL, 2.0×10^8 CFU per mL, and 4.0×10^8 CFU per mL of *Bifidobacterium animalis* subsp. *lactis* BLa80 in a volume of 0.2 mL for the whole one-week period (as depicted in Fig. S1†). The gavage doses of probiotics were meticulously determined at 5-fold, 10-fold, and 20-fold the recommended human consumption level of 1.7×10^8 CFU per kg.[27] When converted to the dosage suitable for a 20-gram mouse, they were 2.0×10^7 CFU, 4.0×10^7 CFU, and 8.0×10^7 CFU respectively.

Throughout the animal experiments, the alterations in the body weight of the mice were documented and monitored on a daily basis. All mice were euthanized on the 15th day. Prior to the conclusion of the experiment, fresh fecal samples were meticulously gathered right after the mice defecated and promptly frozen in a −80 °C refrigerator. On the final day of the experiment, the mice were fasted without water for 12 hours. Orbital blood was drawn from each mouse and left to stand for one hour, after which the collected blood was centrifuged at 4000*g* for 15 min to procure serum for biochemical assays. Subsequently, the mice were sacrificed by cervical dislocation, and the colon tissue was immediately harvested for histopathological analysis and real-time quantitative PCR.

All animal procedures were executed in compliance with the Guidelines for the Care and Use of Laboratory Animals of Tianjin University of Science and Technology. The study was sanctioned by the Institutional Animal Care and Use Committee of Tianjin University of Science and Technology (2022010) [SYXK(Tianjin): 2019-0002].

Measurement of constipation indices

With the intention of closely observing and comprehensively evaluating particular aspects related to the gastrointestinal motility function and fecal characteristics of the mice, specific constipation indices such as fecal water content, small intestinal propulsion rate, and the time taken for the first black stool appearance were determined.

On the 14th day of the experimental process, the mice in each group underwent a 12-hour fasting schedule (with free water supply) and then were given 0.2 mL of an activated charcoal mixture (containing 5% activated charcoal powder and 10% gum arabic) through gavage. Subsequently, each individual mouse was placed into a separate cage, and the precise moment when the first black fecal matter was excreted was meticulously recorded with a timer (RuiXin Biotech Ltd, Quanzhou, China) and defined as the time to the first black stool for the mice (min). The newly collected mouse feces were weighed and marked as the fecal wet weight W_1 (mg). After that, the fecal pellets were placed in a constant temperature oven (Tianjin Zhonghuan Experimental Electric Furnace Ltd., Tianjin, China) set at 105 °C and dried until a fixed weight was achieved, which was recorded as the fecal dry weight W_2 (mg). The formula for computing fecal water content was as follows:

$$\text{Fecal water content } (\%) = [(W_1 - W_2)/W_1] \times 100$$

On the 15th day of the experiment, the small intestinal propulsion rate of the mice was evaluated by measuring the length of ink movement after a 12-hour fasting period, in line with previous research method.[28] All mice were administered 0.2 mL of the aforementioned activated charcoal solution *via* gavage. Precisely 25 minutes after the gavage operation, the animals were euthanized through decapitation. Subsequently, their abdominal cavities were opened using anatomical forceps. Then, the mesentery was carefully dissected with tweezers, and the segment of the intestinal tube stretching from the pylorus to the ileum was excised with a scalpel. The

excised intestinal tube was then carefully positioned on a flat and sterile tray and meticulously straightened, with every effort made to minimize any stretching or twisting of the intestinal tube. The complete length of the intestinal tube was precisely measured and recorded as the "total length of the small intestine" (designated as L_1, cm). At the same time, the distance extending from the pylorus to the foremost edge of the ink was carefully measured and regarded as the "advancement length of the ink" (denoted as L_2, cm). The ratio of L_2 to L_1, expressed as a percentage (L_2/L_1%), functioned as a crucial indicator for the evaluation of the small intestinal propulsion rate.

Histological analysis of the distal colon tissue

In order to investigate the potential influence of the probiotic BLa80 on the integrity of the intestinal barrier in constipated mice, a comprehensive histological analysis was conducted on the tissue of the distal colon tissue. The colon tissue was precisely cut into 2 cm slices. Subsequently, the slices were immersed in 4% paraformaldehyde solution (v/v, Wuhan Servicebio Technology Co., Ltd, Wuhan, Hubei, China) and fixed for a period exceeding 12 hours to ensure proper preservation of tissue structure. After fixation, the tissue was processed for paraffin embedding following standard histological procedures. Paraffin sections were then carefully prepared using a microtome (HistoCore MULTICUT, Leica Microsystems Shanghai Co., Ltd, Shanghai, China), with a thickness of approximately 4 μm. The cut sections were floated in a 40–42 °C warm water bath for natural unfolding. Next, the unfolded sections were retrieved with glass slides and made to adhere. Subsequently, the glass slides were positioned on a 42–45 °C constant temperature stage and baked for several hours to firmly attach the sections. The sections were then twice placed in xylene for 10 minutes each to dewax and remove paraffin. Then the samples were subjected to hematoxylin and eosin (H&E) staining. Firstly, the sections were dewaxed and rehydrated by being successively immersed in 70%, 80%, 90%, 95%, and 100% alcohol solutions (v/v, Sinopharm Group Chemical reagent Co., Ltd) for 2 minutes each. Subsequently, a distilled water rinse was carried out. Then, the sections were subjected to hematoxylin (Wuhan Servicebio Technology Co., Ltd, Wuhan, Hubei, China) staining for 10 min, which led to the cell nuclei being stained blue. After staining, differentiation was carried out using 1% hydrochloric acid in ethanol (v/v, Sinopharm Group Chemical reagent Co., Ltd) for about 5 seconds. The purpose of this was to remove the excess hematoxylin dye on the cell nuclei and make the staining of the cell nuclei clearer. After differentiation, the sections were rinsed with running water and warm water for blueing back, enabling the cell nuclei to present a vivid blue-purple color. After rinsing, the sections were counterstained with eosin (v/v, Wuhan Servicebio Technology Co., Ltd, Wuhan, Hubei, China) for approximately 3 min, which imparted a pink color to the cytoplasm and extracellular matrix. Finally, the sections were dehydrated once more, cleared in xylene (Sinopharm Chemical Reagent Co., Ltd, Beijing, China) twice with each time lasting for 8 minutes, and then mounted with a coverslip. The stained sections were then observed under a biological tissue section processing analysis system, specifically a fluorescence microscope (BX53, Olympus (China) Co., Ltd, Beijing, China), 50 μm, to assess the integrity of the intestinal barrier. The morphology of the colon tissues, including the shape, size, and arrangement of cells within the crypts and the presence and appearance of cup cells, the thickness of the colonic mucus layer, number of intestinal villi, *etc.* were carefully examined and any differences between experimental groups and control groups were noted and documented for further analysis.

Biochemical assays of serum levels of gastrointestinal regulatory peptides

It aimd to understand the roles and potential changes in regulating gastrointestinal functions in mice with constipation, the concentrations of peptides including motilin (MTL), gastrin (GAS), substance P (SP), 5-hydroxytryptamine (5-HT), endothelin (ET-1), growth inhibitor (SS), and vasoactive intestinal peptide (VIP) in the serum were determined in accordance with the instructions of the enzyme-linked immunosorbent assay (ELISA) kit (RuiXin Biotech Ltd, Quanzhou, China).

For the quantification of the gastrointestinal regulatory peptides, 50 μL of the diluted serum (with a final dilution factor of 5 times) was carefully dispensed into the wells of the ELISA plate that had been pre-coated with specific antibodies against MTL, GAS, SP, 5-HT, ET-1, SS, and VIP. Subsequently, the plate was gently agitated to ensure homogeneous mixing. Meanwhile, precisely 50 μL of the standard substance was accurately pipetted into the corresponding wells of the enzyme-labeled coated plate. Additionally, blank wells were established, in which neither samples nor enzyme-labeled reagents were introduced, serving as a control for baseline comparison and to account for any background interference or non-specific binding that might occur during the assay process.

The plate was incubated at 37 °C for 30 min to allow the antigen–antibody reaction to occur. After incubation, the wells were washed five times with washing liquid to remove unbound substances. Then, except for the blank well, a secondary antibody conjugated with horseradish peroxidase (HRP) was added to each well and incubated for another 30 min at 37 °C. The wells were washed five times with washing liquid to remove unbound substances. Subsequently, a color developer solution of 50 μL (usually tetramethylbenzidine, TMB) was added, and the color reaction was allowed to develop in the dark for 10 minutes at 37 °C. The reaction was stopped by adding a stop solution (such as sulfuric acid), and the absorbance at 450 nm was measured immediately using the enzyme labeling instrument (RuiXin Biotech Ltd., Quanzhou, China).

To guarantee the reproducibility and precision of the experimental outcomes, each sample was assayed in triplicate, and the average value was subsequently computed. A standard curve was generated by utilizing a range of known concentrations of the corresponding standards furnished in the

ELISA kit. The concentration of every analyte within the mouse serum was then ascertained by contrasting the absorbance value of the sample with that of the standard curve. After obtaining the measured concentration, calculate the concentration of the sample and multiply it by the dilution factor. The final product is the actual concentration of the sample.

Determination of the short-chain fatty acids (SCFAs) concentration in feces

For the objective of discerning the potential of the probiotic strain to engender beneficial fermentation within the gut lumen, the fluctuation in the generation of short-chain fatty acids (SCFAs) was scrupulously gauged through gas chromatography-mass spectrometry (GC-MS) analysis.[29]

The feces samples were prepared according to the previous method.[29] Accurately measure 30 mg of feces using a precision analytical balance with thousandth percentile accuracy (BS224S, Beijing Sartorius Instrument Systems Co., Ltd, Beijing, China). Resuspend the feces in 500 μL of saturated NaCl solution and ensure thorough mixing by applying a gentle vortexing action using a mixing device (QL-901, Jiangsu Haimen Qilin Bell Instrument Manufacturing Co., Ltd., Nantong, Jiangsu, China). This process may assist in dissociating SCFAs from the fecal matrix and establishing a suitable ionic environment. Following acidification with 20 μL of 10% H_2SO_4, 800 μL of ether was incorporated into the mixture. Then, the mixture was agitated for 10 minutes by a mechanical shaker (HNY-100D, Tianjin Ono Instrument Co., Ltd, Tianjin, China) for the purpose of separating SCFAs from other fecal constituents. Subsequently, the mixture was subjected to centrifugation at 18 000*g* for 15 minutes, thereby segregating the ether phase, which harbored the extracted SCFAs, from the aqueous phase. The upper ether layer was meticulously collected and subsequently introduced into 0.25 g of anhydrous Na_2SO_4. The resultant mixture was left undisturbed for 30 min to eradicate any residual water that might potentially disrupt the GC-MS analysis. Thereafter, the mixture was centrifuged at 18 000*g* for 5 minutes to separate Na_2SO_4 from the ether phase. The clear, dry ether phase containing SCFAs was then primed and ready for injection into the GC-MS system.

The GC-MS (ISQ 7000, Thermo Fisher Scientific (Shanghai) Instrument Co., Ltd, Shanghai, China) analysis is performed on an SH-PolarWax-MS column (SHIMADZU Ltd, USA) with a length of 30 m and an inner diameter of 0.25 μm. Helium (He) is employed as the carrier gas at a flow rate of 1 mL min^{-1}, facilitating stable and reproducible separations. A 1 μL sample was injected into the column with a split ratio of 10 : 1. The injection temperature is set at 240 °C to ensure the complete vaporization of the sample while avoiding thermal degradation of the SCFAs. The column temperature was increased following a specific procedure. It was initiated at 100 °C and then raised to 140 °C at a rate of 7.5 °C min^{-1}. Subsequently, it was increased to 200 °C at a rate of 60 °C min^{-1} and maintained at that temperature for 3 min. The ionization temperature was set at 220 °C. At this temperature, the SCFAs in the gas phase were ionized in the ion source of the mass spectrometer and then detected and analyzed by the mass spectrometer. The analysis was conducted in full scan mode to detect all ions generated from the SCFAs. Finally, the concentration of each short-chain fatty acid (expressed in μmol g^{-1}) within the fecal samples was precisely calculated by means of the peak areas of both the standards and the samples. Afterwards, the purity and concentration of DNA were detected by 1% agarose gel electrophoresis. And the sample DNA was transferred into a centrifuge tube and then diluted to a concentration of 1 ng μL^{-1} using sterile water.

16S rRNA sequencing of gut microbiota in fecal samples

The mouse fecal samples (200 mg) were collected in a sterile manner and immediately stored at −80 °C to preserve the integrity of the microbial DNA until extraction. The fecal samples were thoroughly homogenized by means of a mortar and pestle to guarantee a uniform distribution of the microbial cells and enhance the efficiency of DNA extraction. Subsequently, with the aid of an ultra clean fecal DNA isolation kit (Mo Bio Laboratories Inc, USA), the microbial cells present in the fecal samples were lysed, consequently leading to the release of the genomic DNA. The 16S rDNA V3–V4 hypervariable regions of all bacteria in the samples were sequenced using the Mi Seq Illumina sequencing platform (Illumina, Inc., USA) to characterize the gut microbiota.

Following sequencing, the raw sequence data underwent processing. The raw sequences underwent a series of processing steps, including primer removal, quality filtering, denoising, splicing, and chimera detection. After quality control, each non-redundant sequence generated was designated as an ASV (amplicon sequence variant). These ASVs were then annotated using the Greengenes database Silva version 138.1. A rapid multiple sequence alignment was carried out using the QIIIME2 software to acquire the phylogenetic relationships of all ASVs sequences. The species abundances of each sample at different taxonomic levels were calculated by normalizing the data of each sample. Subsequently, the species abundance information was used to generate heatmaps, Venn diagrams, and other visualizations.

The alpha diversity (such as Shannon index, Chao 1 index, Simpson index, observed_otu index) to assess the diversity within each sample, and beta diversity (such as non metric multidimensional analysis, NMDS) were calculated to compare the differences between samples.[30] Linear discriminant analysis (LDA) was conducted to pinpoint the microbial taxa that exhibited the highest discriminatory power among different groups.[31] Correlations between the dominant bacterial phyla and physiological indices were examined through Spearman correlation analysis.

Real-time quantitative polymerase chain reaction (RT-qPCR) experiment targeting the colon tissues

To analyze the molecular mechanisms underlying the impact of BLa80 on colon-related gene expression in constipated mice, including aquaporin 3 (AQP3), intestinal mucin 2 (MUC2), stem cell factor (SCF) and c-Kit, the RT-qPCR experi-

ment was carried out targeting the colon tissues on a CFX connect real-time PCR system (BioRad, USA). Specifically, the colon tissues of 300 mg were meticulously harvested from the constipated mice that had been treated with BLa80, as well as from those in the control groups and the model group. Total RNA was then extracted from these colon tissues through homogenization in a cracking buffer RLS (with 50 × DTT solution added) of 600 μL supplied in the steadypure universal RNA extraction kit II (Accurate Biotechnology (Hunan) Co., Ltd, Changsha, China). In a 1.5 mL centrifuge tube (RNase free), the mixture was repeatedly pipetted until there was no obvious precipitate in the lysis buffer. The lysis buffer was allowed to stand at room temperature for 2 min. Then, it was centrifuged at 12 000 rpm and 4 °C for 5 min. The supernatant was carefully aspirated into a new 1.5 mL centrifuge tube (RNase free). Subsequently, an equal volume of 70% ethanol was added to the tissue lysate. The mixture was then pipetted up and down to ensure homogeneity until no obvious viscosity or precipitate was observed. After homogenization, the sample was subjected to a universal RNA mini column (Accurate Biotechnology (Hunan) Co., Ltd, Changsha, China), and a series of centrifugation and washing steps as the kit instructions. The high-quality RNA was recovered by performing an elution step with 100 μL of RNase-free water for 5 min. Subsequently, the sample was centrifuged at 12 000 rpm at room temperature for 2 min to elute the RNA (NanoDrop One, Thermo Fisher Scientific (Shanghai) Instrument Co., Ltd, Shanghai, China). Only when this ratio fell within the optimal range of 1.8 to 2.0 was the RNA sample deemed suitable for use in the subsequent steps of the experiment.

These separated qualified was converted into complementary DNA (cDNA) using a Evo M-MLV reverse transcription premix kit II (Accurate Biotechnology (Hunan) Co., Ltd, Changsha, China). The reaction was carried out under specific temperature conditions. First, DNA genome removal step was carried out at around 42 °C for 2 min to synthesize complementary DNA (cDNA) from the isolated RNA while eliminating any contaminating genomic DNA. Then, the reverse transcription step was carried out at around 37 °C for a 15 min, during which the reverse transcriptase synthesizes the cDNA strand complementary to the RNA template. Finally, a heat inactivation step was carried out at approximately 85 °C for 5 seconds, thus getting the cDNA ready for the subsequent procedures.

The cDNA amplification was conducted using the SYBR® Green Premix Pro Taq HS qPCR kit (code. AG11701, Accurate Biotechnology (Hunan) Co., Ltd, Changsha, China) on the CFX connect real-time PCR system. To prepare the reaction mixture, 100 ng of cDNA template samples were added, along with 0.2 μM forward and reverse primers specific for each target gene, namely β-actin (internal reference gene, GAPDH), AQP3, MUC2, SCF and c-Kit. The SYBR green premix, which contains Taq polymerase, dNTPs, $MgCl_2$, and the SYBR green dye, was also incorporated. The primer sequences employed to evaluate the expression of specific colon-related genes were as detailed in Table S1 of the ESI.† The CFX connect real-time PCR system was utilized to execute the thermal cycling. The cycling conditions comprised an initial denaturation step at approximately 95 °C for 30 seconds to ensure complete denaturation of the DNA. Subsequently, 40 amplification cycles were carried out, with each cycle consisting of a denaturation step at around 95 °C for 5 seconds and an annealing step of each primer pair at 60 °C for 30 seconds. Following the amplification cycles, a melting curve analysis was carried out to verify the specificity of the amplified product.

The threshold cycle values (Ct values) were ascertained for each sample and each target gene. The relative expression of the genes was computed by means of the 2-ΔΔCT method. Firstly, the ΔCT value for each target gene was obtained by deducting the Ct value of the GAPDH from the Ct value of the target gene. Subsequently, the ΔΔCT value was determined by subtracting the ΔCT value of the control group from the ΔCT value of the experimental group. Eventually, the relative expression of the target gene was calculated as 2-ΔΔCT.

Statistical analysis

Experimental data were meticulously analyzed and processed with the aid of IBM SPSS statistical software version 26 and GraphPad Prism 9.0 software. The data were presented in the form of mean ± standard deviation (SD). To identify differences among groups, one-way analysis of variance (ANOVA) in conjunction with Duncan's multiple range test was employed. A p-value less than 0.05 was regarded as statistically significant, thereby denoting a meaningful distinction between the groups under investigation.

Results and discussion

The impact of BLa80 treatment on body weight and gastrointestinal motility in mice with constipation

The effects of BLa80 on the physiological and fecal conditions of constipated mice were assessed through body weight, fecal water content, small intestinal propulsion rate, and the time to the first appearance of black stool. Fig. 1A illustrated the pattern of body weight alterations in each group of mice. It was evident that following loperamide treatment, the body weights of mice in each group were substantially lower than those of the blank control group (BC group, $p < 0.05$), indicating that the loperamide treatment impeded weight gain. Loperamide, which acts on the gastrointestinal tract and affects intestinal motility and function, slows the normal intestinal movement in mice. This alters digestion and absorption, preventing efficient nutrient uptake. As proper absorption of proteins, carbs, and fats is essential for weight gain, the disrupted absorption due to loperamide's effect on the intestine hinders normal weight increase.[28] As expected, by day 7 after BLa80 and mosapride citrate tablets (PC group) treatment, the body weights of the mice commenced a gradual recovery. The weight recovery effect was pronounced ($p < 0.05$) in the PC group and all BLa80 dose groups (BLa80-L, BLa80-M and BLa80-H groups) when compared to the model group (M group). This might be attributed to the enhancing effect that

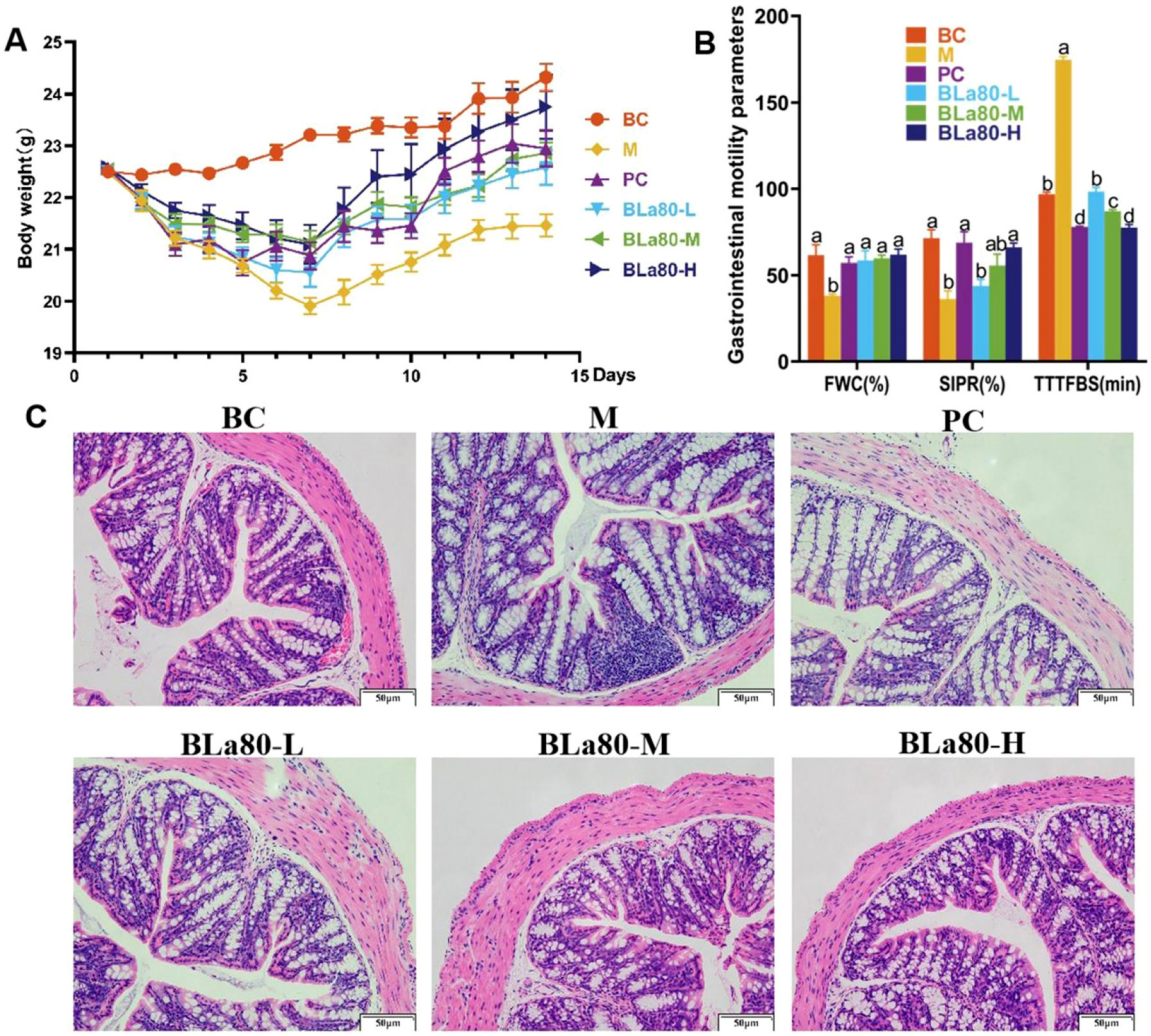

Fig. 1 Impact of Bla80 treatment on body weight, gastrointestinal motility and colonic histomorphology in constipated mice. A, Alterations in body weight. B, The fecal water content (FWC), small intestinal propulsion rate (SIPR), and the time when black stool first appears (TTTFBS). Data were presented as the mean ± SD (n = 10). Different letters signify significant differences among distinct groups, with $p < 0.05$. The different letters represent significant differences between different groups, $p < 0.05$. C, Histopathological examination of the colon *via* hematoxylin & eosin (H&E) staining at a magnification of 100×.

mosapride citrate tablets exert on the motility of the gastrointestinal tract, or the beneficial influence of the probiotic BLa80 on the gut microbiota and gut environment.[32] Such effects could generate a more conducive condition for the digestion and absorption of specific nutrients, thereby promoting a restoration to normal weight gain patterns following the alleviation of constipation-related problems.

The outcomes of fecal water content, small intestinal propulsion rate and the time to the first black stool for the mice are presented in Fig. 1B. In contrast to the BC group, the fecal water content and small intestinal propulsion rate of the mice in the M group were markedly diminished ($p < 0.05$). Nevertheless, the time to the first black stool in constipated mice from the M group was the highest. In comparison to the M group, the fecal water content and small intestinal propulsion rate were notably enhanced, with significantly abbreviated time to the first black stool for the mice in BLa80 treatment groups ($p < 0.05$), especially for the mice treated with BLa80 of high dose. These parameters were comparable in the BC, PC and BLa80-H groups. The results demonstrated that BLa80 was capable of augmenting fecal wetness, accelerating intestinal peristalsis, and enhancing the small intestine propulsion rate, which in turn effectively mitigated constipation. The enhanced motility or the ameliorated gut environment expedites fecal passage, diminishes the time of fecal retention in the colon, precludes excessive water absorption from feces, and consequently gives rise to softer stools and more effortless defecation.

The disparities in the intestinal morphological characteristics among constipated mice

The integrity of the intestinal barrier constitutes a crucial factor in the assessment of the severity of constipation.

Additionally, any damage inflicted upon the intestinal barrier also exerts a varying degree of influence on the peristaltic function of the intestines. To gain a deeper understanding of the role of BLa80 in alleviating the impairment of the gut barrier in constipated mice, the histological staining on the distal end of the mouse colon distal tissue to evaluate the intestinal morphology were conducted. The results, as presented in Fig. 1C, indicated that in the BC group, the small intestinal tissue exhibited an intact structure. The cells within the lamina propria were orderly arranged and structurally distinct, the mucosa and smooth muscle layers were well-organized, and the epithelial layer was continuous without any defects. In contrast, the M group manifested a partial loss of the crypt structure in the colonic mucosal layer and intestinal villi, accompanied by focal inflammatory cell infiltration, a partial reduction in goblet cells, and a diminished thickness of the mucosal and muscular layers. This implied that constipation caused damage to the intestinal barrier, which could be attributed to the increased intraluminal pressure, prolonged contact with toxins, and imbalanced gut microbiota *etc.* induced by constipation.[33] However, following treatment with mosapride citrate tablets and BLa80, the intestinal structure was restored to varying extents. Mice in the BLa80 groups demonstrated a significant reduction in colonic tissue damage, a decline in inflammatory cell infiltration, an increase in the number of goblet cells and intestinal villi, a restoration of the thickness of the colonic mucus layer, an improvement in the cellular condition with a tendency towards normalization, and colonic characteristics that closely resembled those of the BC and PC groups. These observations of colon tissue sections evidently illustrated that BLa80 was proficient in effectively reversing the colon injury instigated by loperamide. This could predominantly be attributed to its multiple beneficial actions. Specifically, BLa80 strengthens tight-junction function, crucial for intestinal epithelial barrier integrity. Tight-junction proteins such as occludin, claudins, and zonula occludens-1 regulate paracellular permeability. By enhancing their expression and localization, BLa80 curbs harmful substance leakage from the gut lumen, alleviating intestinal inflammation. *In vitro*, BLa80 treatment up-regulated occludin and claudin-1 in cell monolayers, reducing dextran passage, signifying a tightened barrier.[34] BLa80 also could promote mucus production. Mucus, rich in mucins, forms a protective layer on the intestinal epithelium, acting as a dual-action pathogen barrier. In animal models, BLa80-mediated mucin increase led to a thicker layer, trapping pathogens and fostering a beneficial-bacteria-friendly environment.[35] Moreover, BLa80 modulates the intestinal cytokine profile. It boosts anti-inflammatory cytokines like IL-10 and TGF-β while reducing pro-inflammatory TNF-α and IL-6 *etc*. In a murine colitis model, BLa80 administration increased IL-10 and TGF-β levels, decreased TNF-α and IL-6, dampening the inflammatory response.[36] BLa80 competitively inhibits pathogenic bacteria. It occupies adhesion sites and synthesizes bacteriocins with broad-spectrum activity against pathogens like *E. coli* and *Salmonella*. By out-competing them, BLa80 curbs pathogen colonization and invasion.[37] Additionally, BLa80 contributes to producing beneficial metabolites such as short-chain fatty acids (SCFAs) and B-vitamins. SCFAs, especially butyrate, are colonocyte energy sources with anti-inflammatory effects.[38] B-vitamins like biotin, folate, and cobalamin, produced by BLa80, are crucial for restoring colon tissue health and integrity.[39] For example, some B-vitamins partake in antioxidant defense, lessening oxidative stress and inflammation. They also affect the gut microbiota, spurring beneficial bacteria growth, safeguarding the intestinal barrier, and blocking pathogen invasion. Previous studies have also demonstrated that *Bifidobacterium lactis* TY-S01 exhibits anti-inflammatory characteristics and fortifies the integrity of the gastrointestinal mucosal barrier.[40] Consequently, BLa80 might prove efficacious in ameliorating the symptoms of constipation by facilitating the restoration of intestinal damage in constipated mice.

The alteration of the serum levels of gastrointestinal regulatory peptides in different groups of mice

The outcomes regarding the levels of gastrointestinal regulatory peptides were presented in Fig. 2A and Table 1. Gastrointestinal hormones, which are small-molecule peptides, have been identified as significant mediators within the gut–brain axis. This axis serves as a crucial link, interconnecting the enteric nervous system (ENS) of the gastrointestinal tract and the central nervous system (CNS).[41] It is within this context that the gastrointestinal regulatory peptides associated with constipation could play a vital role in regulating gastrointestinal motility and brain–gut connection. Among them, motilin (MTL), gastrin (GAS) and substance P (SP) acted as excitatory transmitters for promoting gastrointestinal motility, whereas endothelin-1 (ET-1), growth suppressor (SS) and vasoactive intestinal peptide (VIP) acted as inhibitory transmitters for reducing gastrointestinal motility. As shown in Fig. 2A, in the M group, the contents of gastrointestinal regulatory peptides such as MTL, GAS, SP, and 5-hydroxytryptamine (5-HT) were significantly lower than those in the BC group ($p < 0.05$), indicating loperamide hydrochloride's inhibitory effect on them in constipated mice. This indicated loperamide reduced the release of the peptides involved in promoting gastrointestinal motility.[42] The results also showed that the levels of ET-1, SS, and VIP were remarkably increased in the M group compared with the BC group, with statistically significant differences ($p < 0.05$). The rise in ET-1, SS and VIP could be a regulatory mechanism to balance the changes caused by the loperamide-induced reduction in motility.[40] These observation was consistent with previous findings in constipated mice, which showed lower serum levels of MTL, GAS, and SP and higher levels of ET-1, SS, and VIP.[43]

Subsequent to treatment with different doses of BLa80 or mosapride citrate tablets, all groups exhibited varying degrees of recovery. Specifically, in the groups that were administered different doses of BLa80, the MTL, Gas, SP, and 5-HT contents were considerably higher in comparison to the M group ($p < 0.05$). The ET-1, SS, and VIP contents were significantly lower in the PC group as well as in the groups with different doses of

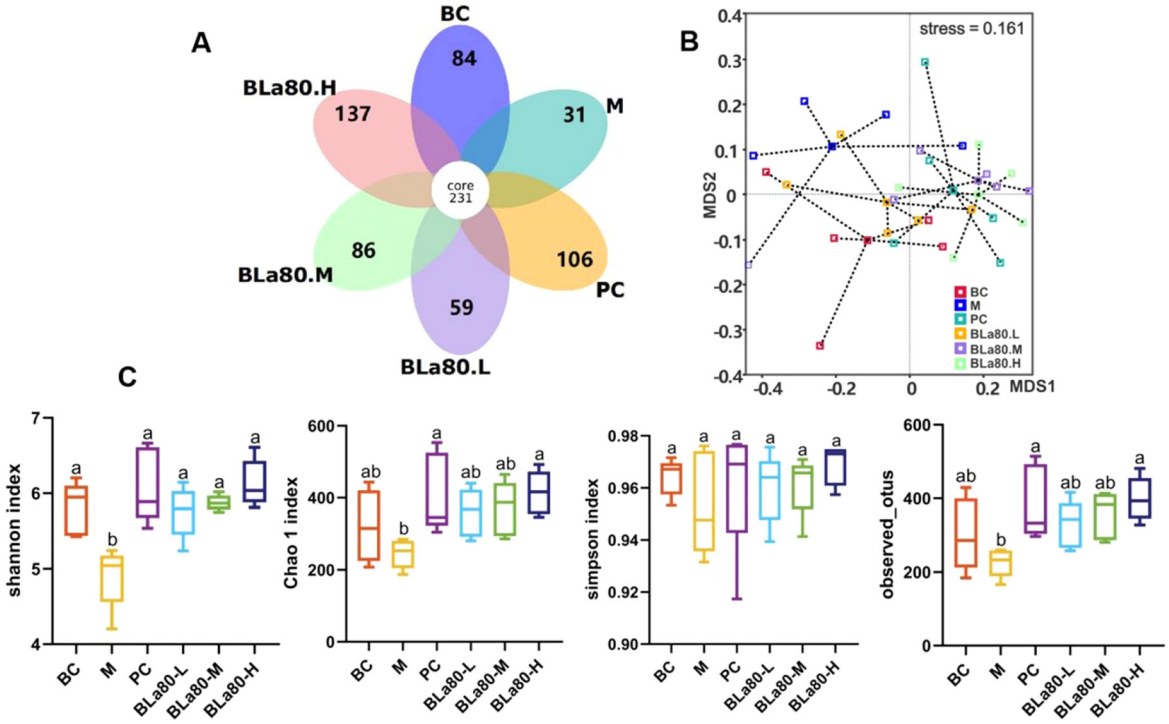

Fig. 2 Effect of BLa80 administration on gut microbiota composition and diversity. A, Venn diagram of the interspecific overlap of mice in each group. B, β-Diversity analysis based on NMDS (stress = 0.161). C, The Shannon index, Chao 1 index, Simpson index, and observed_otus index. Data are expressed as mean or mean ± SD (n = 10). The different letters represent significant differences between different groups, $p < 0.05$.

BLa80 when contrasted with the M group ($p < 0.05$). These results indicated that BLa80 was capable of effectively enhancing the secretion of MTL, Gas, SP and 5-HT, while simultaneously reducing the secretion of ET-1, SS and VIP.

The variation in the levels of these peptides could be explained from multiple perspectives. Loperamide hydrochloride, which functions as the opioid receptor agonist within the enteric nervous system (ENS), is capable of binding to specific receptors in the gastrointestinal tract. This binding interaction triggers a cascade of modifications in neurotransmitter release and regulatory mechanisms, thereby modulating the secretion of gastrointestinal regulatory peptides.[44] BLa80 as a probiotic, could interact with the ENS and immune cells in the gut, which played a crucial role in the release of gastrointestinal regulatory peptides. Probiotics can prevent an overactive immune response that may increase ET-1, SS and VIP. ET-1 is well-known for its role in vasoconstriction and can also contribute to inflammation in the gut.[45] SS has inhibitory effects on various physiological processes in the gut, and an excessive amount of it can disrupt normal gut function.[41] VIP, can cause abnormal fluid secretion and relaxation of smooth muscles in the gut, which can further affect digestion and absorption.[46] By modulating the immune system and maintaining a proper balance, probiotics act as a safeguard to prevent the overproduction of ET-1, SS and VIP, thereby promoting an optimal digestive function. For beneficial peptides like MTL, Gas, SP, and 5-HT, probiotics enhance immune-mediated signals for gut endocrine cells. These interactions boost peptide production and release, aiding gastrointestinal motility. Additionally, probiotics, by enhancing the barrier function and out-competing the pathogens, can restore a healthy gut environment. Simultaneously, a healthy gut environment fostered by probiotics is conducive to the normal endocrine function of the gut and augments the communication between epithelial cells and endocrine cells. This, in turn, results in an elevated secretion of MTL, Gas, SP and 5-HT.

The variation in the concentration of short-chain fatty acids (SCFAs) within the feces of mice

To verify whether BLa80 has an impact on gut microbial metabolites, the contents of acetic acid, propionic acid, isobutyric acid, butyric acid, isovaleric acid, valeric acid, and total short-chain fatty acids (SCFAs) in the feces were determined. The results indicated that the level of SCFAs in the feces of mice in different dosage groups of BLa80 was significantly elevated compared with mice in the MC group that received loperamide treatment. With the exception of isobutyric acid and isovaleric acid, the levels of other SCFAs in the mice of the M group were markedly lower than those in the BC group ($p < 0.05$, Fig. 2B). Nevertheless, the concentrations of acetic acid, propionic acid, butyric acid, valeric acid, and total SCFAs were significantly elevated in the PC group and the various dose groups of BLa80 ($p < 0.05$). Notably, the amounts of acetic

Table 1 The serum concentrations of gastrointestinal regulatory peptides and the feces contents of short-chain fatty acids (SCFAs) in various groups of mice

	Group					
Index	BC	M	PC	BLa80-L	BLa80-M	BLa80-H
Serum levels of gastrointestinal regulatory-related peptides						
MTL	355.33 ± 9.72^{a}	281.45 ± 12.30^{d}	338.415 ± 7.20^{b}	309.715 ± 8.99^{c}	322.72 ± 11.30^{c}	346.205 ± 10.76^{ab}
GAS	190.77 ± 6.35^{a}	152.035 ± 6.16^{d}	180.315 ± 8.68^{b}	162.765 ± 5.85^{c}	173.265 ± 5.33^{b}	192.075 ± 3.54^{a}
SP	213.795 ± 8.22^{a}	130.09 ± 8.21^{e}	197.84 ± 6.35^{b}	150.765 ± 6.15^{d}	159.35 ± 6.67^{d}	184.885 ± 5.99^{c}
5-HT	180.295 ± 8.06^{a}	73.015 ± 2.53^{d}	175.515 ± 6.17^{a}	124.13 ± 4.30^{c}	127.51 ± 4.53^{c}	140.3 ± 7.61^{b}
ET-1	90.31 ± 5.10^{b}	104.59 ± 4.81^{a}	91.87 ± 3.25^{b}	89.51 ± 2.88^{b}	80.42 ± 3.06^{c}	75.39 ± 3.85^{c}
SS	334.42 ± 4.37^{de}	412.455 ± 7.66^{a}	325.785 ± 6.63^{e}	381.765 ± 7.33^{b}	360.21 ± 6.74^{c}	337.48 ± 5.48^{d}
VIP	369.955 ± 12.87^{b}	479.445 ± 12.24^{a}	309.395 ± 8.62^{d}	368.31 ± 14.70^{b}	357.99 ± 17.17^{b}	334.765 ± 13.59^{c}
Fecal SCFAs composition						
Acetic acid	63.85 ± 1.36^{a}	17.77 ± 1.10^{d}	57.28 ± 0.66^{b}	41.59 ± 0.97^{c}	54.00 ± 0.60^{b}	62.63 ± 1.50^{ab}
Propionic acid	21.67 ± 1.36^{a}	6.88 ± 1.00^{d}	15.97 ± 1.51^{b}	9.58 ± 1.01^{c}	12.71 ± 1.46^{c}	13.85 ± 0.76^{bc}
Butanoic acid	12.06 ± 1.21^{a}	5.04 ± 0.67^{c}	10.12 ± 0.33^{ab}	7.71 ± 0.62^{b}	8.45 ± 0.88^{b}	9.72 ± 1.00^{ab}
Isobutyric acid	8.27 ± 1.08^{ab}	5.48 ± 1.27^{b}	7.83 ± 0.60^{ab}	6.44 ± 1.20^{b}	8.40 ± 0.55^{ab}	9.85 ± 1.06^{a}
Valeric acid	4.52 ± 1.05^{a}	1.54 ± 0.37^{b}	4.03 ± 0.95^{a}	3.83 ± 0.61^{a}	4.77 ± 0.65^{a}	5.39 ± 1.11^{a}
Isovaleric acid	9.28 ± 1.25^{a}	2.86 ± 0.39^{bc}	5.34 ± 0.56^{b}	5.13 ± 1.02^{bc}	6.34 ± 0.58^{b}	8.09 ± 0.87^{ab}
Total SCFAs	119.65 ± 1.91^{a}	39.57 ± 2.17^{f}	100.56 ± 0.48^{c}	74.28 ± 0.39^{e}	94.67 ± 2.85^{d}	109.53 ± 1.57^{b}

Data represent the mean ± SD (n = 10). Different letters within the same row denote significant differences among distinct groups, with a significance level of $p < 0.05$.

acid, butyric acid, isobutyric acid, valeric acid, and isovaleric acid were restored to the values of the blank control (BC group) in the BLa80-H group. However, the content of propionic acid and total SCFAs exhibit a significant decrease (Table 1).

SCFAs are crucial metabolites of the intestinal microbiota and a significant mediator within the gut–brain axis. The SCFAs actuate intestinal mucosal receptors and the vagus nerve, which directly influence colonic smooth muscle to propel peristalsis.[47] SCFAs constitute an essential target for exploring the correlation between intestinal microbiota and constipation.[16] Moreover, they curtail the intestinal transit time by augmenting intestinal 5-HT concentrations, thereby alleviating the symptoms of constipation. Multiple studies have indicated that probiotics can sustain the level of SCFAs in the intestine and consequently maintain regular bowel movements.[48] Additionally, SCFAs are assimilated by colonic epithelial cells and also function as an energy reservoir. They maintain the physiological function and normal morphology of intestinal cells by diminishing the osmotic pressure of the intestinal cells, thus reducing the absorption of water from feces by the intestinal lumen. High osmotic pressure can have an adverse impact on intestinal cells.[49] It appeared to be corroborated by the results of the fecal water content, which was significantly increased in BLa80-treated mice. It is postulated that this is closely related to the rise in SCFAs within the intestine. Furthermore, SCFAs are capable of suppressing inflammation and safeguarding the integrity of the intestinal epithelium, thereby enhancing the frequency of gastrointestinal motility. This aligns with the outcomes regarding the timing of the first black stool and intestinal morphology mentioned above.[50] Previous investigations have established that SCFAs could stimulate the secretion of peptides related to the regulation of the gastrointestinal tract to stimulate gastrointestinal peristalsis, which coincides with the alterations in the levels of gastrointestinal regulatory peptides in the present study.[13]

The impact of BLa80 treatment on the composition and diversity of the intestinal microbiota

Given the key role of intestinal bacterial ecology in constipation, this study probed the changes in composition and diversity of the intestinal microbiota of constipated mice (Fig. 3). As shown in the Venn diagram (Fig. 3A), 258 Amplicon Sequence Variant (ASV) were shared among the six sample groups. Namely, 83 ASV were unique to the BC group, 31 to the M group, 108 to the PC group, 57 to the BLa80-L group, 85 to the BLa80-M group, and 134 to the BLa80-H group. Among them, the M group had a notably lower ASV count than the others, indicating a significant reduction in species specific to the gut microbiota of loperamide-induced constipated mice.[51] In contrast, the BLa80-H group had a much higher ASV number, suggesting BLa80 treatment greatly increased the species specific to the gut microbiota of such constipated mice.

The NMSD plot is presented in Fig. 3B. It clearly demonstrated a distinct separation in the gut microbiota between the BC and M groups. This implied that the gut microbiota of the mice in the M group underwent alterations following loperamide intervention and was substantially different from those of the BC group. The gut microbiota samples of BLa80-L group mice partially overlap with those of M group. This indicated that the low-dose BLa80 did not bring about a significant enhancement in the gut microbiota of the mice subjected to loperamide interference. The samples of mice in the PC and BLa80-M groups hardly overlapped with those of the mice in the M group at all. This suggested that mosapride citrate tablets and medium-dose BLa80 did improve the intestinal microbiota of constipated mice. The samples of the mice in

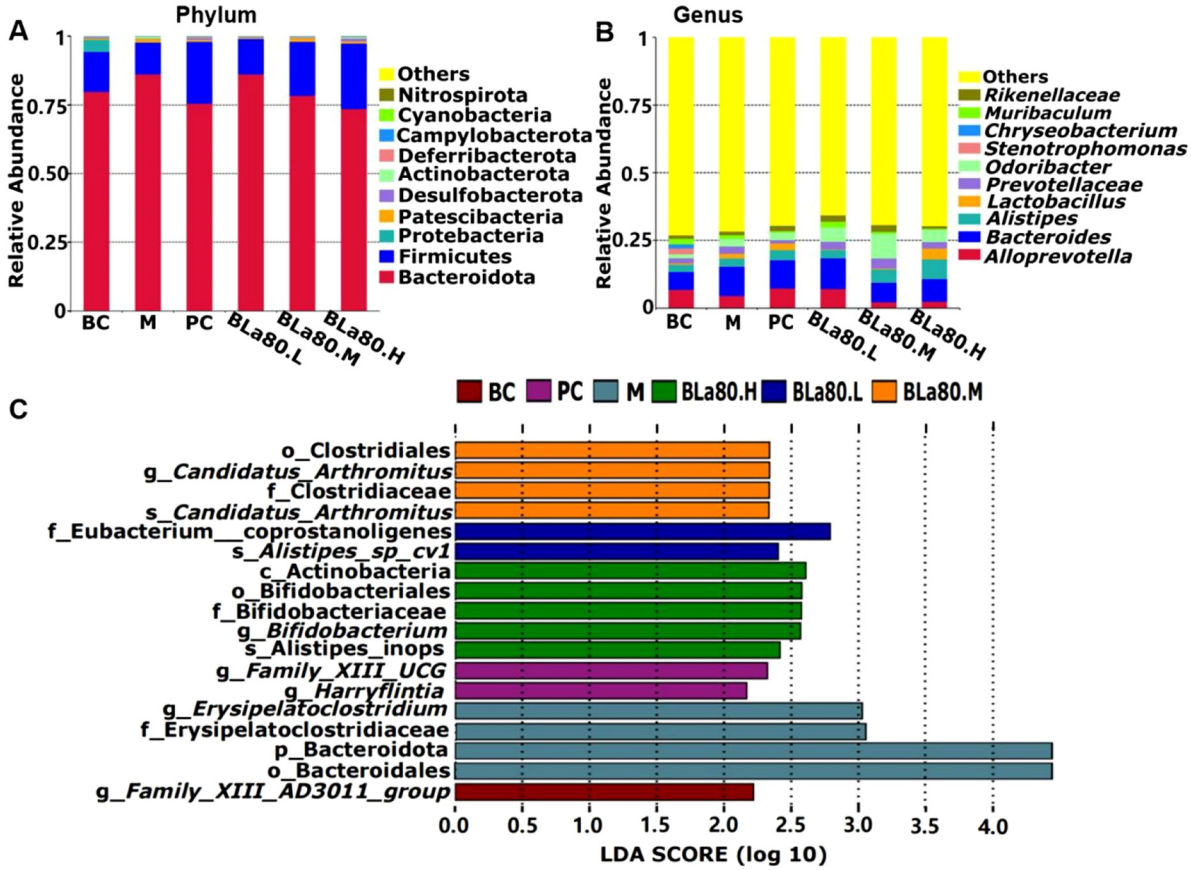

Fig. 3 Differences in intestinal microbiota composition at the phylum and genus levels. A, The alterations of the microbial community structure at the phylum level. B, The alterations of the microbial community structure at the genus level. C, The LDA score of the microbiota among different groups. Data are expressed as mean (n = 10).

the BLa80-H group were separated from the sample points of the other groups and were in close proximity to those of the BC group. This implied that the high-dose BLa80 managed to shift the gut microbiota of constipated mice towards the BC group to a certain degree.[52]

Alpha diversity analysis was indicative of the diversity and richness of gut microbiota in mice. The Shannon index, Chao 1 index, Simpson index, and observed_otus index were positively correlated with the relative abundance of gut microorganisms in mice. The results are presented in Fig. 3C. In comparison with the M group, the Shannon index, Chao 1 index, and observed_otus index of the BC, PC, BLa80-L, BLa80-M, and BLa80-H groups were significantly augmented ($p < 0.05$), signifying an increase in the diversity or richness of the intestinal microbiota. This implied that BLa80 was capable of ameliorating constipation by modulating the intestinal microbiota and enhancing the intestinal microecological environment. There was no significant difference in Simpson's index among the groups, suggesting that these treatments had a minimal impact on the relative abundance of dominant species for microbial communities.[53]

For a more in-depth exploration of the impact of BLa80 on the intestinal microbiota of loperamide-induced constipated mice, analyses were carried out at the phylum and genus levels, respectively. The results are presented in Fig. 4A and B. At the phylum level (Fig. 4A), the microbiota of the mouse gut was predominantly constituted by Bacteroidetes and Firmicutes. In response to loperamide, the relative abundance of Bacteroidetes significantly rose in the M group (Fig. 4C), while that of Firmicutes declined, compared with the other groups. This led to a high Bacteroidetes-to-Firmicutes (B : F) ratio (M : 7.42; BC : 5.50; PC : 3.37; BLa80-L : 6.67; BLa80-M : 4.01; BLa80-H : 3.09), which implied lower energy absorption. This was consistent with the results of the previous analysis on body weight gain. Nevertheless, following the intervention of different doses of BLa80, the structure of the gut microbiota in all groups was reversed to varying extents, with a particularly significant effect observed in the BLa80-H group. At the genus level (Fig. 4B), compared with the BC group, the abundance of *Alloprevotella* diminished in the M group. *Alloprevotella*, a major butyrate producer, inhibits intestinal pathogens and benefits host health. In mice treated with loperamide hydrochloride, the abundance of *Alloprevotella* declined, directly reducing intestinal butyrate production. The decrease in butyrate may attenuate pathogen inhibition and impact the overall health of the mice.[54]

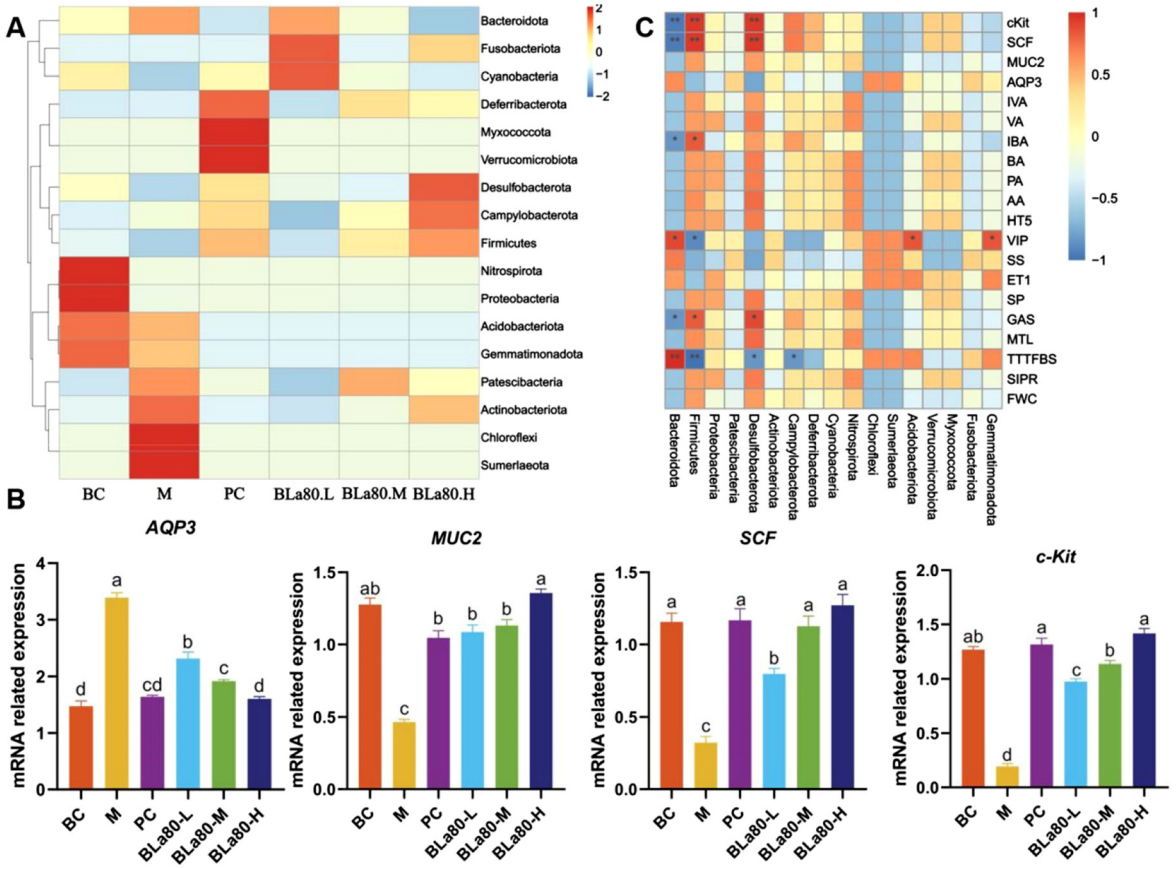

Fig. 4 The dominating bacteria at phylum level and expression of corresponding genes in the colon. A, The relative abundance of the top 20 species at the phylum level. B, mRNA expression levels of AQP3, MUC2, SCF and c-kit in the colon of constipated mice. Data are presented as the mean ± SD (n = 10). Different letters denote significant differences among different groups, with $p < 0.05$. C, Spearman's correlation between the dominant bacteria at the phylum level and physiological indices. The colors of squares represent the R-value of Spearman's correlation.

Concurrently, the relative abundances of *Alistipes*, *Odoribacter* and *Rikenellaceae* in the BLa80 groups were observably higher compared with those in the M group (Fig. 4B). Moreover, the abundance of *Bifidobacterium* was significantly higher than that in the other groups (LDA ≥ 2, Fig. 4C). The augmentation of these bacteria was prone to result in an elevation of beneficial metabolites such as SCFAs. Subsequently, this could activate specific signaling pathways within the host and impact the secretion of gastrointestinal hormones *via* an indirect effect on the intestinal environment.[55] For example, *Alitipes*, anaerobic colonizers of the human gut, are linked to intestinal health. They degrade and ferment fiber to produce butyric acid *etc.*, crucial for colon health as it powers colon cells, preserves mucosal integrity, and regulates inflammation.[56] *Odoribacter*, belonging to the phylum Bacteroidetes, like Alitipes, aids SCFAs production and intestinal health, diminishing inflammation and colon cancer risk.[57] *Rikenellaceae*, which is implicated in lipid and amino acid metabolism and the formation of SCFAs, shows a correlation with acids such as butyric and valeric.[58] Conversely, within the M group, certain harmful bacteria, exemplified by *Erysipelatoclostridium*, exhibited a significant enrichment (LDA ≥ 2, Fig. 4C). *Erysipelatoclostridium* is often associated with gut dysbiosis. Certain species can generate toxins, which damage intestinal epithelial cells crucial for nutrient uptake and serving as a shield. Damaged epithelium causes enhanced intestinal permeability ("leaky gut"), permitting toxins and undigested matter to access the bloodstream and potentially instigate systemic inflammation and immune reactions. In poultry, it may result in retarded growth, inefficient feed conversion, and elevated mortality.

Furthermore, a heat map analysis was conducted on the relative abundance of the top 20 species at the phylum level to evaluate the distribution of gut microbes among each group of mice. The results are presented in Fig. 4A. In the BC group mice, the abundances of Nitrospirota, Proteobacteria, Acidobacteriota, and Actinobacteriota were relatively high. It was observed that the dominant genera in group M were mainly concentrated in Acidobacteriata, Gemmatimonadota, Patescibacteria, Actinobacteriota, Chloroflexi, and Sumerlaeota. In contrast, in the BLa80 group mice, there was an increase in Bacteroidota, Fusobacteroidota, Cynaobacteria, Patescibacteria, Desulfobacterota, Campylobacterota, Firmicutes, and Actinobacteriota. Meanwhile, the PC group mice exhibited an enrichment of Deferribacterota, Myxococcota, and Verrucomicrobiota. Generally speaking, the

microbiota composition of the BLa80 group differed remarkably from that of the M group, and the structure of the gut microbiota in BLa80-treated mice was more akin to that of the PC group. Some harmful bacteria were significantly enriched in group M. For example, Sumerlaeota and Chloroflexi. These are not the main components of the gut microbiota, but changes in their quantities may have an impact on human health when there is an imbalance in the gut microbiota.[59] For instance, when people suffer from intestinal diseases that lead to the disorder of the gut microbiota, Sumerlaeota and Chloroflexi may take the opportunity to multiply in large numbers. Such changes may trigger intestinal inflammatory responses, because their metabolic products may irritate the intestinal mucosa or change the chemical environment within the intestine, thus affecting the normal physiological functions of the intestine. These findings imply that BLa80 modulated the imbalance of the intestinal microbiota in constipated mice by facilitating the growth of beneficial bacteria and suppressing the proliferation of harmful bacteria, thereby contributing to the restoration of intestinal homeostasis and the alleviation of constipation.

Expression of corresponding genes in the colon among distinct groups of mice

The results of the effect of BLa80 on the expression of colon-related genes in constipated mice, which were analyzed by RT-qPCR, are presented in Fig. 4B. The obtained results demonstrated that the mRNA expression of AQP3 was notably higher in the M group in contrast to the BC group ($p < 0.05$). Conversely, the mRNA expression of MUC2, SCF, and c-Kit was significantly lower in the M group ($p < 0.05$). This probable be one of the main reasons for the decrease in fecal water content and fecal dryness in the distal colon. And it could be accounted for by the competitive water absorption in the colon, the decline of the hydrogel mucus barrier, the augmented quantity of ICC, along with the elevated expression of AQPs, the repressed expressions of MUC2, and the SCF/c-Kit signaling pathway.[60–62] When compared with the M group, the mRNA expression levels of AQP3 in the PC group and different dose groups of BLa80 were decreased to a more significant extent ($p < 0.05$). Meanwhile, the mRNA expression levels of MUC2, SCF, and c-Kit in the PC and different dose groups of BLa80 were increased more remarkably ($p < 0.05$), with the alterations being more prominent in the BLa80-H group. This suggested that BLa80 treatment could moderately reduce the competitive water absorption in the colon, enhanced the intestinal barrier function, and augmented the expression levels of the SCF/c-Kit pathway, thereby enhancing gastrointestinal motility and alleviating the symptoms of constipation. BLa80 treatment promoted the colonization of more beneficial bacteria, which could secrete bioactive factors or beneficial metabolites such as SCFAs. These bioactive factors or beneficial metabolites could reduce the excessive water-absorbing capacity of the colon by regulating the functions of epithelial cells and tight junctions, and also stimulate the production of mucus-secreting goblet cells. Moreover, the beneficial bacteria is capable of participating in the regulation of ICCs by interacting with the gut epithelium and the enteric nervous system, enhancing the expression of c-Kit and its ligand SCF, and the activation of this pathway can strengthen intestinal motility.[62]

The outcomes of the Spearman correlation coefficient among the composition of the intestinal microbiota, the gastrointestinal motility indices, the serum levels of gastrointestinal regulatory peptides, the SCFAs levels within the feces of mice, and expression of corresponding genes are illustrated in Fig. 4C. Specifically, Bacteroidata, Acidobacteriota, and Gemmatimonadota, which had relatively high abundances in the mice of the M group, exhibited a notably positive correlation with the first black stool time and the level of the gastrointestinal regulatory peptide VIP ($p < 0.05$ or $p < 0.01$). Conversely, they demonstrated a significantly negative correlation with the levels of GAS, isobutyric acid, and the mRNA expression levels of SCF and c-Kit ($p < 0.05$ or $p < 0.01$). Firmicutes and Desulfobacteriota, having relatively high abundances in the mice of the BLa80 groups, presented a remarkably positive correlation with the levels of GAS, isobutyric acid, and the mRNA expression levels of SCF and c-Kit ($p < 0.05$ or $p < 0.01$), and a significantly negative correlation with the first black stool time and VIP level ($p < 0.05$ or $p < 0.01$). Consequently, it could speculated that BLa80 is capable of alleviating constipation symptoms by augmenting the abundance of intestinal bacteria that are positively associated with constipation-relieving metabolites and further enhancing parameters such as the first black stool time, SCFAs, gastrointestinal regulatory peptides, and mRNA expression levels.

Conclusion

The groundbreaking and pioneering study conducted a comprehensive and in-depth analysis of the effects of BLa80 on loperamide-induced constipation in mice from a diverse range of perspectives, including feces-related parameters, serum neurotransmitters, short-chain fatty acids (SCFAs), gene levels, protein levels, and intestinal microbiota. It was uncovered that BLa80 significantly increased the fecal water content, actively promoted intestinal peristalsis, and remarkably enhanced the propulsion rate of the small intestine in constipated mice. Moreover, our research results clearly demonstrated that BLa80 had the ability to modulate the level of gastrointestinal regulatory-related peptides, effectively raise the content of SCFAs, robustly upregulate the gene expression of gastrointestinal-related proteins, successfully relieve intestinal inflammation, and stably maintain the homeostasis of the intestinal microbiota, thus leading to a transformation in intestinal function. As a result, BLa80 could proficiently and effectively alleviate loperamide-induced constipation in mice and potentially emerges as a highly promising and prospective alternative for the treatment of constipation. Looking forward, these findings offer hope. Future studies could explore BLa80's long-term safety and efficacy in more diverse models or human trials, potentially making it a widely available treatment. It may also inspire new drug development for this common disorder.

Author contributions

Zhaochun Zhang, the first author, made significant contributions to this work, and was responsible for conceptualization, data curation, formal analysis, investigation, writing the initial draft and revision, *etc*. Jie Li, Ziyi Wan, Shuguang Fang, and Yunjiao Zhao, corresponded for the investigation, data curation and formal analysis. Qian Li and Min Zhang, corresponded for the project administration, and supervision.

Data availability

The data that support the findings of this study are available from the corresponding author upon reasonable request. The data supporting this article have been included as part of the ESI.†

Conflicts of interest

The authors have declared no conflict of interest.

Acknowledgements

This work was supported by the project of Natural Science Foundation of Tianjin Municipality (no. 24JCQNJC00740), 2024 Tianjin "the Belt and Road" Innovation Platform Project (no. 24PTLYHZ00020), the Key Research and Development Program of China (no. 2022YFF1100201).

We would like to express our sincere gratitude to Wecare Probiotics Co., Ltd for their invaluable support in terms of materials and funding.

References

1 R. Venkataraman, R. Shenoy, J. J. Ahire, J. Neelamraju and R. S. Madempudi, Effect of *Bacillus coagulans unique IS2* with lactulose on functional constipation in adults: a double-blind placebo controlled study, *Probiotics Antimicrob. Proteins*, 2023, **15**, 379–386.

2 B. Barberio, C. Judge, E. V. Savarino and A. C. Ford, Global prevalence of functional constipation according to the rome criteria: a systematic review and meta-analysis, *Lancet Gastroenterol. Hepatol.*, 2021, **6**, 638–648.

3 X. L. Zeng, L. J. Zhu and X. D. Yang, Exploration of the complex origins of primary constipation, *World J. Clin. Cases*, 2024, **12**, 5476–5482.

4 V. Oliva, M. Lippi, R. Paci, L. Del Fabro, G. Delvecchio, P. Brambilla, D. De Ronchi, G. Fanelli and A. Serretti, Gastrointestinal side effects associated with antidepressant treatments in patients with major depressive disorder: a systematic review and meta-analysis, *Prog. Neuro-Psychopharmacol.*, 2021, **109**, 110266.

5 G. S. Sayuk, S. A. Waldman and D. M. Brenner, Mechanisms of action of current pharmacologic options for the treatment of chronic idiopathic constipation and irritable bowel syndrome with constipation, *Am. J. Gastroenterol.*, 2022, **117**, S6–S13.

6 S. S. C. Rao and D. M. Brenner, Efficacy and safety of over-the-counter therapies for chronic constipation: an updated systematic review, *Am. J. Gastroenterol.*, 2021, **116**, 1156–1181.

7 A. K. Sinha, M. F. Laursen, J. E. Brinck, M. L. Rybtke, A. P. Hjørne, N. Procházková, M. Pedersen, H. M. Roager and T. R. Licht, Dietary fibre directs microbial tryptophan metabolism via metabolic interactions in the gut microbiota, *Nat. Microbiol.*, 2024, **9**, 1964–1978.

8 Q. Huang, F. Yu, D. Liao and J. Xia, Microbiota-immune system interactions in human neurological disorders, *CNS Neurol. Disord.: Drug Targets*, 2020, **19**, 509–526.

9 K. Alagiakrishnan and T. Halverson, Microbial therapeutics in neurocognitive and psychiatric disorders, *J. Clin. Med. Res.*, 2021, **13**, 439–459.

10 M. Muhammad, S. Muchimapura and J. Wattanathorn, Microbiota-gut-brain axis impairment in the pathogenesis of stroke: implication as a potent therapeutic target, *Biosci. Microbiota, Food Health*, 2023, **42**, 143–151.

11 M. Hagbom, A. Hellysaz, C. Istrate, J. Nordgren, S. Sharma, F. M. de-Faria, K. E. Magnusson and L. Svensson, The 5-HT (3) receptor affects rotavirus-induced motility, *J. Virol.*, 2021, **95**, e0075121.

12 F. H. Login and L. N. Nejsum, Aquaporin water channels: roles beyond renal water handling, *Nat. Rev. Nephrol.*, 2023, **19**, 604–618.

13 Z. Yang, S. Ye, Z. Xu, H. Su, X. Tian, B. Han, B. Shen, Q. Liao, Z. Xie and Y. Hong, Dietary synbiotic ameliorates constipation through the modulation of gut microbiota and its metabolic function, *Food Res. Int.*, 2021, **147**, 110569.

14 J. D. Huizinga, A. Hussain and J. H. Chen, Interstitial cells of cajal and human colon motility in health and disease, *Am. J. Physiol.: Gastrointest. Liver Physiol.*, 2021, **321**, G552–G575.

15 Y. Li, Y. Yu, X. Wu, B. Liu, H. Ma, X. Zhao, S. Cao, S. Ding, T. Li, X. Wang, P. Wang, X. Xu, J. Zhao, Y. Liu, C. Lan, J. Wang, L. Chen and Q. Zeng, Applied nutritional investigation specially designed yogurt supplemented with combination of pro- and prebiotics relieved constipation in mice and humans, *Nutrition*, 2022, **103–104**, 111802.

16 L. Wang, S. Cen, G. Wang, Y. K. Lee and W. Chen, Acetic acid and butyric acid released in large intestine play different roles in the alleviation of constipation, *J. Funct. Foods*, 2020, **69**, 103953.

17 M. Yu, B. Yu and D. Chen, The effects of gut microbiota on appetite regulation and the underlying mechanisms, *Gut Microbes*, 2024, **16**, 2414796.

18 J. Eastwood, G. Walton, S. Van Hemert, C. Williams and D. Lamport, The effect of probiotics on cognitive function across the human lifespan: a systematic review, *Neurosci. Biobehav. Rev.*, 2021, **128**, 311–327.

19 J. Y. Kim, J. Y. Kim, H. Kim, E. C. Moon, K. Heo, J. J. Shim and J. L. Lee, Immunostimulatory effects of dairy probiotic

strains *Bifidobacterium animalis* ssp. *Lactis* HY8002 and *Lactobacillus plantarum*, HY7717, *J. Anim. Sci. Technol.*, 2022, **64**, 1117–1131.

20 Y. Xindi, L. Weichen, F. Haihong, H. Jiaqiang, W. Qi, Z. Qi, H. Jingjing and W. Ran, *Bifidobacterium animalis* subsp. *Lactis*, A6 attenuates hippocampal damage and memory impairments in an adhd rat model, *Food Funct.*, 2024, **15**, 2668–2678.

21 P. Xu, K. Cui, L. Chen, S. Chen and Z. Wang, Effect of dietary *Bifidobacterium animalis*, subsp. *Lactis* BLa80 on growth, immune response, antioxidant capacity, and intestinal microbiota of juvenile japanese seabass (*lateolabrax japonicus*), *Aquacult. Int.*, 2023, **32**, 1749–1769.

22 L. J. Myhill, S. Stolzenbach, H. Mejer, L. Krych, S. R. Jakobsen, W. Kot, K. Skovgaard, N. Canibe, P. Nejsum, D. S. Nielsen, S. M. Thamsborg and A. R. Williams, Parasite-probiotic interactions in the gut: *Bacillus* sp. and *Enterococcus faecium* regulate type-2 inflammatory responses and modify the gut microbiota of pigs during helminth infection, *Front. Immunol.*, 2021, **12**, 793260.

23 L. Wang, L. Wang, P. Tian, B. Wang, S. Cui, J. Zhao, H. Zhang, L. Qian, Q. Wang, W. Chen and G. Wang, A randomised, double-blind, placebo-controlled trial of *Bifidobacterium bifidum* CCFM16 for manipulation of the gut microbiota and relief from chronic constipation, *Food Funct.*, 2022, **13**, 1628–1640.

24 M. B. La Monica, B. Raub, H. L. Lopez and T. N. Ziegenfuss, A probiotic amylase blend reduces gastrointestinal symptoms in a randomised clinical study, *Benefic. Microbes*, 2023, **14**, 459–476.

25 T. Ma, X. Shen, X. Shi, H. A. Sakandar, K. Quan, Y. Li, H. Jin, L.-Y. Kwok, H. Zhang and Z. Sun, Targeting gut microbiota and metabolism as the major probiotic mechanism - An evidence-based review, *Trends Food Sci. Technol.*, 2023, **138**, 178–198.

26 L. C. Beck, A. C. Masi, G. R. Young, T. Vatanen, C. A. Lamb, R. Smith, J. Coxhead, A. Butler, B. J. Marsland, N. D. Embleton, J. E. Berrington and C. J. Stewart, Strain-specific impacts of probiotics are a significant driver of gut microbiome development in very preterm infants, *Nat. Microbiol.*, 2022, **7**, 1525–1535.

27 X. Zhou, Y. Chen, X. Ma, Y. Yu, X. Yu, X. Chen and H. Suo, Efficacy of *Bacillus coagulans* BC01 on loperamide hydrochloride-induced constipation model in kunming mice, *Front. Nutr.*, 2022, **9**, 964257.

28 X. Zhang, J. Zheng, N. Jiang, G. Sun and H. Liu, Modulation of gut microbiota and intestinal metabolites by lactulose improves loperamide-induced constipation in mice, *Eur. J. Pharm. Sci.*, 2021, **158**, 105676.

29 L. H. Chen, S. S. Chang, H. Y. Chang, C. H. Wu, C. H. Pan, C. C. Chang, C. H. Chan and H. Y. Huang, Probiotic supplementation attenuates age-related sarcopenia via the gut-muscle axis in SAMP8 mice, *J. Cachexia Sarcopeni Muscle*, 2022, **13**, 515–531.

30 J. A. F. Westaway, R. Huerlimann, Y. Kandasamy, C. M. Miller, R. Norton, D. Watson, S. Infante-Vilamil and D. Rudd, To probiotic or not to probiotic: a metagenomic comparison of the discharge gut microbiome of infants supplemented with probiotics in nicu and those who are not, *Front. Pediatr.*, 2022, **10**, 838559.

31 D. Suga, H. Mizutani, S. Fukui, M. Kobayashi, Y. Shimada, Y. Nakazawa, Y. Nishiura, Y. Kawasaki, I. Moritani, Y. Yamanaka, H. Inoue, E. Ojima, Y. Mohri, H. Nakagawa, K. Dohi, K. Takaba, H. Wada and K. Shiraki, The gut microbiota composition in patients with right- and left-sided colorectal cancer and after curative colectomy, as analyzed by 16s rRNA gene amplicon sequencing, *BMC Gastroenterol.*, 2022, **22**, 313.

32 M. Y. Lee, M. S. Kim and Y. S. Kim, Intracolonic administration of mosapride citrate significantly increases colonic motility compared with oral administration, *J. Neurogastroenterol.*, 2023, **29**, 265.

33 Y. Chen, L. Zhang, Y. Zhang, T. Bai, J. Song, W. Qian and X. Hou, Ephrina1/Epha2 promotes epithelial hyperpermeability involving in lipopolysaccharide-induced intestinal barrier dysfunction, *J. Neurogastroenterol.*, 2020, **26**, 397–409.

34 P. Zhang, Influence of foods and nutrition on the gut microbiome and implications for intestinal health, *Int. J. Mol. Sci.*, 2022, **23**, 9588.

35 G. Pereira-Caro, S. Cáceres-Jiménez, A. Moreno-Ortega, S. Dobani, K. Pourshahidi, C. I. R. Gill, P. Mena, D. Del Rio, J. M. Moreno-Rojas, G. Taurino, O. Bussolati, T. M. Almutairi, A. Crozier and M. G. Bianchi, Colon-available mango (poly)phenols exhibit mitigating effects on the intestinal barrier function in human intestinal cell monolayers under inflammatory conditions, *Food Funct.*, 2024, **15**, 5118–5131.

36 Y. Dong, W. Liao, J. Tang, T. Fei, Z. Gai and M. Han, *Bifidobacterium* BLa80 mitigates colitis by altering gut microbiota and alleviating inflammation, *AMB Express*, 2022, **12**, 67.

37 X. Ding, Z. Liu, Y. Liu, B. Xu, J. Chen, J. Pu, D. Wu, H. Yu, C. Jin and X. Wang, Comprehensive evaluation of the mechanism of gastrodia elata blume in ameliorating cerebral ischemia-reperfusion injury based on integrating fecal metabonomics and 16s rDNA sequencing, *Front. Cell. Infect. Microbiol.*, 2022, **12**, 1026627.

38 H. Xia, J. Guo, J. Shen, S. Jiang, S. Han and L. Li, Butyrate ameliorated the intestinal barrier dysfunction and attenuated acute pancreatitis in mice fed with ketogenic diet, *Life Sci.*, 2023, **334**, 122188.

39 E. Simon, L. F. Călinoiu, L. Mitrea and D. C. Vodnar, Probiotics, prebiotics, and synbiotics: implications and beneficial effects against irritable bowel syndrome, *Nutrients*, 2021, **13**, 2112.

40 T. Tang, J. Wang, Y. Jiang, X. Zhu, Z. Zhang, Y. Wang, X. Shu, Y. Deng and F. Zhang, *Bifidobacterium lactis* TY-S01 prevents loperamide-induced constipation by modulating gut microbiota and its metabolites in mice, *Front. Nutr.*, 2022, **9**, 890314.

41 J. Singh, Vanlallawmzuali, A. Singh, S. Biswal, R. Zomuansangi, C. Lalbiaktluangi, B. P. Singh, P. K. Singh, B. Vellingiri, M. Iyer, H. Ram, B. Udey and

M. K. Yadav, Microbiota-brain axis: exploring the role of gut microbiota in psychiatric disorders - a comprehensive review, *Asian J. Psychiatr.*, 2024, **97**, 104068.

42 T. H. Liu, G. L. Chen, C. H. Lin, T. Y. Tsai and M. C. Cheng, *Lactobacillus plantarum* TWK10 relieves loperamide-induced constipation in rats fed a high-fat diet via modulating enteric neurotransmitters, short-chain fatty acids and gut microbiota, *Food Funct.*, 2025, **16**, 181–194.

43 S. Cheng, B. Li, Y. Ding, B. Hou, W. Hung, J. He, Y. Jiang, Y. Zhang and C. Man, The probiotic fermented milk of *lacticaseibacillus paracasei* JY062 and *lactobacillus gasseri* JM1 alleviates constipation via improving gastrointestinal motility and gut microbiota, *J. Dairy Sci.*, 2024, **107**, 1857–1876.

44 Y. Monu, P. Milind, S. Nidhi, K. J. Deepak, J. Kajal, R. Neha and G. Tinku, Development and evaluation of loperamide hydrochloride loaded chitosan nanoformulation for neurotoxic effects on mice, *Polym. Bull.*, 2024, **81**, 5111–5133.

45 L. Seguella, I. Palenca, S. B. Franzin, A. Zilli and G. Esposito, Mini-review: Interaction between intestinal microbes and enteric glia in health and disease, *Neurosci. Lett.*, 2023, **806**, 137221.

46 Q. Zhao, Y. Y. Chen, D. Q. Xu, S. J. Yue, R. J. Fu, J. Yang, L. M. Xing and Y. P. Tang, Action mode of gut motility, fluid and electrolyte transport in chronic constipation, *Front. Pharmacol.*, 2021, **12**, 630249.

47 H. Li, Y. Xiang, Z. Zhu, W. Wang, Z. Jiang, M. Zhao, S. Cheng, F. Pan, D. Liu, R. C. M. Ho and C. S. H. Ho, Rifaximin-mediated gut microbiota regulation modulates the function of microglia and protects against cums-induced depression-like behaviors in adolescent rat, *J. Neuroinflammation*, 2021, **18**, 254.

48 Q. Xiao-Hang, C. Si-Yue and T. Hui-Dong, Multi-strain probiotics ameliorate Alzheimer's-like cognitive impairment and pathological changes through the AKT/GSK-3β pathway in senescence-accelerated mouse prone 8 mice, *Brain, Behav., Immun.*, 2024, **119**, 14–27.

49 M. Zitek, Z. Celewicz, J. Kikut and M. Szczuko, Implications of SCFAs on the parameters of the lipid and hepatic profile in pregnant women, *Nutrients*, 2021, **13**, 1749.

50 L. Dupraz, A. Magniez, N. Rolhion, M. L. Richard, G. Da Costa, S. Touch, C. Mayeur, J. Planchais, A. Agus, C. Danne, C. Michaudel, M. Spatz, F. Trottein, P. Langella, H. Sokol and M. L. Michel, Gut microbiota-derived short-chain fatty acids regulate IL-17 production by mouse and human intestinal γδ T cells, *Cell Rep.*, 2021, **36**, 109332.

51 X. Gao, W. Yang, S. Li, S. Liu, W. Yang, S. Song, J. Sheng, Y. Zhao and Y. Tian, Moringa oleifera leaf alleviates functional constipation via regulating the gut microbiota and the enteric nervous system in mice, *Front. Microbiol.*, 2023, **14**, 1315402.

52 C. B. Forsyth, M. Shaikh, P. A. Engen, F. Preuss, A. Naqib, B. A. Palmen, S. J. Green, L. Zhang, Z. R. Bogin, K. Lawrence, D. Sharma, G. R. Swanson, F. Bishehsari, R. M. Voigt and A. Keshavarzian, Evidence that the loss of colonic anti-microbial peptides may promote dysbiotic Gram-negative inflammaging-associated bacteria in aging mice, *Front. Aging*, 2024, **5**, 1352299.

53 S. C. Forster, S. Clare, B. S. Beresfordjones, K. Harcourt, G. Notley, M. D. Stares, N. Kumar, A. T. Soderholm, A. Adoum and H. Wong, Identification of gut microbial species linked with disease variability in a widely used mouse model of colitis, *Nat. Microbiol.*, 2022, **7**, 590–599.

54 J. Wei, Y. Zhao, C. Zhou, Q. Zhao, H. Zhong, X. Zhu, T. Fu, L. Pan, Q. Shang and G. Yu, Dietary polysaccharide from enteromorpha clathrata attenuates obesity and increases the intestinal abundance of butyrate-producing bacterium, *eubacterium xylanophilum*, in mice fed a high-fat diet, *Polymers*, 2021, **13**, 3286.

55 I. Huber-Ruano, E. Calvo, J. Mayneris-Perxachs, M. M. Rodríguez-Peña, V. Ceperuelo-Mallafré, L. Cedó, C. Núñez-Roa, J. Miro-Blanch, M. Arnoriaga-Rodríguez, A. Balvay, C. Maudet, P. García-Roves, O. Yanes, S. Rabot, G. M. Grimaud, A. De Prisco, A. Amoruso, J. M. Fernández-Real, J. Vendrell and S. Fernández-Veledo, Orally administered *odoribacter laneu*s, improves glucose control and inflammatory profile in obese mice by depleting circulating succinate, *Microbiome*, 2022, **10**, 135.

56 C. Song, T. Zhang, D. Xu, M. Zhu, S. Mei, B. Zhou, K. Wang, C. Chen, E. Zhu and Z. Cheng, Impact of feeding dried distillers' grains with solubles diet on microbiome and metabolome of ruminal and cecal contents in guanling yellow cattle, *Front. Microbiol.*, 2023, **14**, 1171563.

57 B. S. Oh, W. J. Choi, J. S. Kim, S. W. Ryu, S. Y. Yu, J. S. Lee, S. H. Park, S. W. Kang, J. Lee, W. Y. Jung, Y. M. Kim, J. H. Jeong and J. H. Lee, Cell-free supernatant of *odoribacter* splanchnicus isolated from human feces exhibits anti-colorectal cancer activity, *Front. Microbiol.*, 2021, **12**, 736343.

58 Z. Xie, W. He, A. Gobbi, H. C. Bertram and D. S. Nielsen, The effect of *in vitr*o, simulated colonic ph gradients on microbial activity and metabolite production using common prebiotics as substrates, *BMC Microbiol.*, 2024, **24**, 83.

59 R. Chen, H. L. Wong, G. S. Kindler, F. I. MacLeod, N. Benaud, B. C. Ferrari and B. P. Burns, Discovery of an abundance of biosynthetic gene clusters in shark bay microbial mats, *Front. Microbiol.*, 2020, **11**, 1950.

60 Y. Zhan, X. Tang, H. Xu and S. Tang, Maren pills improve constipation via regulating AQP3 and NF-κB signaling pathway in slow transit constipation *in vitro* and *in vivo*, *J. Evidence-Based Complementary Altern. Med.*, 2020, **2020**, 9837384.

61 S. Pandey, Exploring the interaction between MUC2 and intestinal signaling molecules using molecular dynamics simulations, *Biophys. J.*, 2024, **123**, 544a.

62 T. Li, Q. Yan, Y. Wen, J. Liu, J. Sun and Z. Jiang, Synbiotic yogurt containing konjac mannan oligosaccharides and *Bifidobacterium animalis* ssp. *Lactis* BB12 alleviates constipation in mice by modulating the stem cell factor (SCF)/c-Kit pathway and gut microbiota, *J. Dairy Sci.*, 2021, **104**, 5239–5255.

